Science Bulletin 67 (2022) 448–451

Contents lists available at ScienceDirect

Science Bulletin

journal homepage: www.elsevier.com/locate/scib

News & Views

Connectome Computation System: 2015–2021 updates

Xiu-Xia Xing [a,*], Ting Xu [b], Chao Jiang [c], Yin-Shan Wang [d,e,f], Xi-Nian Zuo [d,e,f,*]

[a] Department of Applied Mathematics, College of Mathematics, Faculty of Science, Beijing University of Technology, Beijing 100124, China
[b] Center for the Developing Brain, Child Mind Institute, NY 10022, USA
[c] School of Psychology, Capital Normal University, Beijing 100048, China
[d] State Key Laboratory of Cognitive Neuroscience and Learning, Beijing Normal University, Beijing 100875, China
[e] National Basic Science Data Center, Beijing 100190, China
[f] Developmental Population Neuroscience Research Center, IDG/McGovern Institute for Brain Research, Beijing Normal University, Beijing 100875, China

The Connectome Computation System (CCS) was previously reported in the *Science Bulletin* [1]. Here, we describe a summary of the 6-year CCS updates (2015–2021), which are accessible at https://github.com/zuoxinian/CCS. These updates contain many utilities of mining developmental neuroimaging data. Specifically, H1 module covers the data cleaning and preprocessing and refines the implementations of face-masking, brain extraction, denoising, and frequency banding. H2 module implements the individual connectome mapping and adds functions of mapping walk-based network metrics. H3 module facilitates connectome mining and knowledge discovery and updates the intraclass correlation statistics with linear mixed models as well as introduces normative modeling methods. The CCS also improves the end-user experience through well-documented online instruction on installation and usage. CCS updates all the three (H1, H2, and H3) modules during 2015–2021. We note that only the major updates are documented with details in this article while the comprehensive documents of the CCS updates are accessible online in both English and Chinese (https://github.com/zuoxinian/CCS/tree/master/manual).

In sharing neuroimaging data, the protection of identifiable facial features is of paramount importance. Now, CCS includes the face-masking tool [2], which has been integrated into the Human Connectome Project database (HCP) to anonymize the facial information. We recently demonstrated an effect of head template on the face-making use, indicating a better performance of the facial anonymization with the Chinese head templates than that with the Western templates for obscuring the faces of Chinese brain images, and vice versa. Accordingly, we released the Chinese head templates reconstructed from the Chinese Human Connectome Project (CHCP) [3] and the developing component of the Chinese Color Nest Project (devCCNP) [4] as parts of the CCS updates (https://github.com/zuoxinian/CCS/tree/master/templates).

Accurate brain extraction or skull stripping is critical for quantitative brain imaging analysis, especially for morphological measurements such as cortical thickness and surface area. In the 2015 release, CCS first removed the spatial non-local noise using an adaptive algorithm (SANLM) implemented in MATLAB and then extracted the brain using the FreeSurfer toolkit with some manual tweaks. This has been platform-crossing and time-consuming while an online MRI segmentation system, volBrain integrated the two steps. However, the volBrain's performance on brain extraction was largely influenced by the facial anonymization. The updated CCS employed a deep learning method for brain extraction based on the face-masked data [5]. Of note, multiple U-net models were trained for Chinese pediatric brain extraction (not for other tissue segmentation) using head and brain MRI images (obtained using the semi-automatic skull stripping method) from devCCNP [6]. The new-version CCS combined the SANLM function of ANTS with the brain extraction models to achieve a more integrative pipeline.

Neural oscillations generate rhythms of the brain at multiple frequency bands, which correspond to specific physiological processes, respectively. In the CCS updates, we included an open toolbox with a graphical user interface for decoding rhythms of the brain system (DREAM) [7]. It can precisely compute the number and ranges of decodable frequency bands using the sampling parameters. The new CCS offers DREAM as a reliable and valid tool to discover brain waves from multiple frequency windows of the resting-state functional MRI (rfMRI) signal. As one example, Fig. 1a displays data from the left human amygdala of a single subject from the HCP young adult release.

CCS updates the individual mapping with recent advances on walk-based algorithms for network metrics [8]. We introduced multiple network centrality metrics x based on walks of a brain graph in the original CCS release [1], which can be formulated as a function of the graph's adjacency matrix A [9]. A walk around the graph is any route from node to node that makes use of the available edges. The matrix A provides a convenient way to count walks and thus quantify the graph centrality. The number of walks of length n between node i and node j is the (i-th row, j-th column) element of A^n, i.e., $(A^n)_{ij}$. This walk-based graph fact can be used to derive various network centrality metrics such as degree, subgraph, eigenvector, and page rank. Here, we take the stepwise connectivity as an example of the walk-based method to show how we update the centrality metrics by introducing different types of walks. Specifically, for a given seed node, the n-step connectivity

* Corresponding authors.
E-mail addresses: xingxx@bjut.edu.cn (X.-X. Xing), xinian.zuo@bnu.edu.cn (X.-N. Zuo).

https://doi.org/10.1016/j.scib.2021.11.021

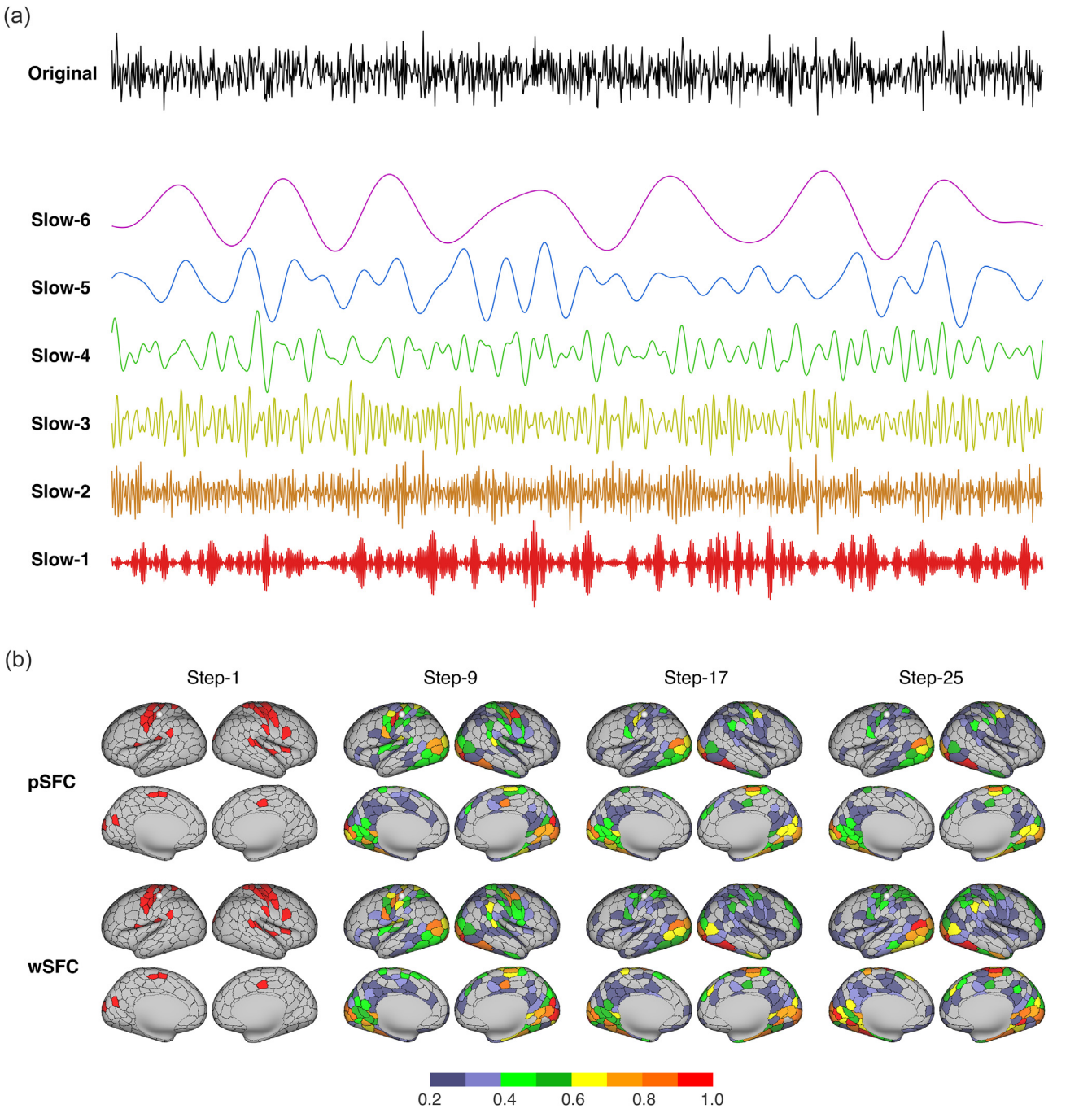

Fig. 1. CCS updates DREAM and network mapping. (a) DREAM, the new utility of CCS, decomposes an original rfMRI signal into the six slow bands: slow-6 (0.0069–0.0116 Hz), slow-5 (0.0116–0.0301 Hz), slow-4 (0.0301–0.0822 Hz), slow-3 (0.0822–0.2234 Hz), slow-2 (0.2234–0.6065 Hz), and slow-1 (0.6065–0.6944 Hz). The original signal is the mean signal across all the voxels within the HCP subject 100160's left amygdala, reflecting the spontaneous brain activity. (b) Stepwise functional connectivity (SFC) was mapped with new CCS functions. Using the 400-parcel cortical parcellation, an adjacency matrix was reconstructed by using the rfMRI signals (in the slow-4 band) from the HCP subject 103818. Based on the matrix, the SFC maps were estimated for both common walks (wSFC) and nonbacktracking walks (pSFC) of lengths of 1, 9, 17, and 25. The walk seed was a parcel in the left sensory motor network (7Network_LH_SomMot_21) [15] and indicated as a white sphere on the cortical surface. All the SFC values are normalized by their maximal value while only SFC greater than 0.2 are shown.

of any other node is the number of walks of length n between this node and the seed node, which has been introduced by Sepulcre et al. [10].

In this release of CCS updates, we constrain the computation with nonbacktracking walks (NBTW), never continuing along the reverse of the edge arrived. This can be implemented by simply replacing the matrix A^n with $p_n(A)$ where $p_0(A) = I$, $p_1(A) = A$, $p_2(A) = A^2 - D$, $p_n(A)$ for $n \geq 3$ satisfy the following four-term recurrence:

$$p_n(A) = p_{n-1}(A)A + p_{n-2}(A)(I - D) - p_{n-3}(A)(A - S), \quad (1)$$

where $d_{ii} = (A^2)_{ii}$ and $s_{ij} = a_{ij}a_{ji}$. We also extended the NBTW computation to its non-cycling version [11]. In Fig. 1b, we demonstrated an individual connectome mapping of stepwise connectivity using the walks derived from A^n and $p_n(A)$, n = 1, 9, 17, and 25 based on the adjacency matrix. We note that the individual connectome mapping is based on the preprocessed rfMRI data in the cortical surface space, which has been advanced by the initial CCS release [1].

Another key CCS update is the reliability module. In this version, CCS offers a selection of intraclass correlation (ICC) models using the Linear Mixed Model (LMM) for assessing measurement reliability. Traditionally, the ICC calculation is defined under the analysis of variance (ANOVA) framework [12,13]—the ratio of the difference between between-subjects mean square (MS_b) and within-subject mean square (MS_w) divided by the sum of MS_b and MS_w. However, when MS_b term is lower than MS_w, the ANOVA approach results in a negative ICC value. To overcome this issue, we adopted the LMM with the restricted maximum likelihood (ReML) estimation method. This guarantees non-negative ICC values and avoids uninterpretable negative estimation under the ANOVA framework. More importantly, the LMM provides the flexibility to handle confounding variables at different levels in the same model (e.g., age, sex at the subject level, and head motion at the session level). Users can thus specify the confounding variables and include them as covariates in the model.

The updated CCS implements all classic types of ICC in one-way random-effects, two-way random-effects, and two-way mixed-effects models. Specifically, ICC(1,1) is estimated in the one-way random-effects model:

$$y = \mu_0 + \lambda_j + \epsilon_{ij}, \qquad \mathrm{ICC}(1,1) = \frac{\sigma_\lambda^2}{\sigma_\lambda^2 + \sigma_\epsilon^2}, \tag{2}$$

where μ_0 is the intercept of the model; λ_j is the random effect of the j-th subject and ϵ_{ij} is the residual. The random variables λ_j and residual ϵ_{ij} are assumed to be independent, in which $\lambda_j \sim N(0, \sigma_\lambda^2)$ and $\epsilon_{ij} \sim N(0, \sigma_\epsilon^2)$. ICC(2,1) is defined as the absolute agreement under the two-way random-effects model:

$$y = \mu_0 + \lambda_j + \alpha_i + \epsilon_{ij}, \qquad \mathrm{ICC}(2,1) = \frac{\sigma_\lambda^2}{\sigma_\lambda^2 + \sigma_\alpha^2 + \sigma_\epsilon^2}, \tag{3}$$

where λ_j and α_i are random effects of the j-th subject and i-th rater (e.g., session). The random variables λ_j, α_i and residual ϵ_{ij} are assumed to be independent, $\lambda_j \sim N(0, \sigma_\lambda^2)$, $\alpha_j \sim N(0, \sigma_\alpha^2)$, $\epsilon_{ij} \sim N(0, \sigma_\epsilon^2)$. ICC(3,1) is defined as the consistency under the two-way mixed-effects model:

$$y = \mu_0 + \lambda_j + \alpha_i + \epsilon_{ij}, \qquad \mathrm{ICC}(3,1) = \frac{\sigma_\lambda^2}{\sigma_\lambda^2 + \sigma_\epsilon^2}. \tag{4}$$

Unlike the two-way random-effects model, here α_i is the fixed effect of the rater. Beyond the explicit types of test–retest design on the measurement reliability assessment (https://github.com/zuoxinian/CCS/tree/master/H3/reliability), CCS offers an online version of the reliability computation, which is no need for predeterminant on the statistical models (http://ibraindata.com/research/reliableFNN/reliabilityassessment).

A normative modeling method (NMM) has been implemented in the updated CCS (https://github.com/zuoxinian/CCS/tree/master/H3/nmm). Such an implementation is inspired by the utility of growth charts in pediatric clinical practice, but generalizable to lifespan brain charts [1,6]. Specifically, given an individual brain metric X, its normative d-score can be derived by overlaying X onto the canonical charts matched to the individual age and sex. Such a score is defined as the norm-version Z-score:

$$d = \frac{2(X - X_{\mathrm{norm}}(50\%))}{X_{\mathrm{norm}}(95\%) - X_{\mathrm{norm}}(50\%)}. \tag{5}$$

With a large representative sample, NMM combines normal participants' information with small-sample studies by controlling effects of both age and sex (other factors as well) in a more realistic manner than with the common methods (e.g., case-control). We demonstrated the promise of using NMM [14] for experimental designs where it is difficult to recruit healthy controls (e.g., rare clinical conditions) by offering a healthy or normal reference and improving the reproducibility of findings. We built a series of growth charts on brain development at school age (6–18 years) and shared via the CCS website (https://github.com/zuoxinian/CCS/tree/master/H3/GrowthCharts).

Conflict of interest

The authors declare that they have no conflict of interest.

Acknowledgments

This work was supported by the Startup Funds for Leading Talents at Beijing Normal University, the National Basic Science Data Center 'Chinese Data-sharing Warehouse for In-vivo Imaging Brain' (NBSDC-DB-15). The neuroimaging data were provided by the HCP WU-Minn Consortium, which is funded by the 16 NIH institutes and centers that support the NIH Blueprint for Neuroscience Research 1U54MH091657 (principal investigators: David Van Essen and Kamil Ugurbil), the McDonnell Center for Systems Neuroscience at Washington University. We thank Dr. Avram Holmes from the Department of Psychology, Yale University for his assistance on proofreading the manuscript.

References

[1] Xu T, Yang Z, Jiang L, et al. A Connectome Computation System for discovery science of brain. Sci Bull 2015;60:86–95.
[2] Milchenko M, Marcus D. Obscuring surface anatomy in volumetric imaging data. Neuroinformatics 2013;11:65–75.
[3] Yang G, Zhou S, Bozek J, et al. Sample sizes and population differences in brain template construction. Neuroimage 2020;206:116318.
[4] Dong HM, Castellanos F, Yang N, et al. Charting brain growth in tandem with brain templates at school age. Sci Bull 2020;65:1924–34.
[5] Wang X, Li XH, Cho J, et al. U-net model for brain extraction: trained on humans for transfer to non-human primates. Neuroimage 2021;235:118001.
[6] Liu S, Wang YS, Zhang Q, et al. Chinese Color Nest Project: an accelerated longitudinal brain-mind cohort. Dev Cogn Neurosci 2021;52:101020.
[7] Gong ZQ, Gao P, Jiang C, et al. DREAM: a toolbox to decode rhythms of the brain system. Neuroinformatics 2021;19:529–45.
[8] Arrigo F, Higham D, Noferini V. A theory for backtrack-downweighted walks. SIAM J Matrix Anal A 2021;42:1229–47.
[9] Estrada E, Higham D. Network properties revealed through matrix functions. SIAM Rev 2010;52:696–714.
[10] Sepulcre J, Sabuncu M, Yeo T, et al. Stepwise connectivity of the modal cortex reveals the multimodal organization of the human brain. J Neurosci 2012;32:10649–61.
[11] Arrigo F, Higham D, Noferini V. Beyond non-backtracking: non-cycling network centrality measures. P Roy Soc A-Math Phy 2020;476:20190653.
[12] Xing XX, Zuo XN. The anatomy of reliability: a must read for future human brain mapping. Sci Bull 2018;63:1606–7.
[13] Koo TK, Li MY. A guideline of selecting and reporting intraclass correlation coefficients for reliability research. J Chiropr Med 2016;135:155–63.
[14] Jia XZ, Zhao N, Dong HM, et al. Small P values may not yield robust findings: an example using REST-meta-PD. Sci Bull 2021;66:2148–52.
[15] Schaefer A, Kong R, Gordon E, et al. Local-global parcellation of the human cerebral cortex from intrinsic functional connectivity MRI. Cereb Cortex 2018;28:3095–114.

Xiu-Xia Xing is an associate professor at the Department of Applied Mathematics, College of Mathematics, Faculty of Science, Beijing University of Technology. She received her B.S., M.S. and Ph.D. degrees from Capital Normal University. Her research interest includes traveling waves arising from biology, chemistry, physics, and mathematical and statistical models of human brain mapping and their applications.

Xi-Nian Zuo is a professor at State Key Laboratory of Cognitive Neuroscience and Learning, Beijing Normal University. He received his B.S. and M.S. degrees from Capital Normal University, and Ph.D. degree from Beijing Normal University. His research interest centers around measurement theory, cohort, and mechanism for developmental population cognitive neuroscience.